Measurement of Deformability of Biological Cell Passing through Single Micro Slit between Walls

Yusuke TAKAHASHI, Shigehiro HASHIMOTO, Atsushi MIZOI, Haruka HINO, Takeshi YAMAGUCHI

Biomedical Engineering, Department of Mechanical Engineering,
Kogakuin University, Tokyo, 163-8677, Japan
http://www.mech.kogakuin.ac.jp/labs/bio/

and

Toshitaka YASUDA

Bio-systems Engineering, Department of Electronic Engineering,
Tokyo National College of Technology, Tokyo, Japan

ABSTRACT

A single micro slit has been designed between walls to observe the deformation of a cell passing through the slit *in vitro*. The micro slit of 0.015 mm width, 0.1 mm length and 0.05 mm height was fabricated between walls of weirs on the glass plate using the photolithography technique. The single micro slit is set in the flow path between parallel plates, of which dimension of the cross section has 2 mm width and 0.05 mm height. Three types of biological cells were used in the test alternatively: C2C12 (mouse myoblast cell line), Hepa1-6 (mouse hepatoma cell line), and Neuro-2a (mouse neural crest-derived cell line). The suspension of cells was introduced into the slits by the pressure difference between the inlet and the outlet, which was kept by the gravitational level of the medium. The cell passing through the slit was observed by the microscope. The movement and the shape of the cell was analyzed at the video images. The elastic modulus of myoblast passing through the slit estimated by the velocity (1 mm/s) and by the deformation ratio (0.5) of the cell in the slit was 10^{-2} Pa. The experimental results show that the designed slit has capability to measure deformability of the cell.

Keywords: Biomedical Engineering, C2C12, Hepa1-6, Neuro2-a, Photolithography and Micro Flow Channel.

1. INTRODUCTION

Biological cells can pass through narrow gaps: micro capillaries, or micro slits. The biological system sorts cells according to the size, deformability, and adsorptivity of the cell. Cells are sorted according to deformability through the gap or adsorptivity on the membrane *in vitro* [1-16]. The technique might be applied to handle cells in diagnostics *in vitro* [17-21].

A red blood cell has flexibility and deforms in the shear flow [22, 23]. It also passes through micro-circulation, of which the dimension is smaller than the diameter of the red blood cell. After circulation through the blood vessels for days, the red blood cell is trapped in the micro-circulation systems. Some cells can pass through the slit narrower than the capillary.

The photolithography technique enables manufacturing a micro-pattern [24-27]. Several micro-fabrication processes have been designed to simulate the morphology of the microcirculation. In the previous study, the micro slits have designed between micro cylindrical pillars [1], or between micro ridges [2]. The micro-fabrication technique has also been applied to design microfluidic systems *in vitro* [3-9].

In the present study, a single micro slit has been designed between walls to observe the deformation of a cell passing through the slit *in vitro*.

2. METHODS

Micro Slit

A single micro slit has been designed between walls of weirs (Fig. 1). The micro slit of 0.015 mm width, 0.1 mm length (L) and 0.05 mm height (H) was fabricated between walls of weirs on the glass plate using the photolithography technique. The single micro slit is set in the flow path between parallel plates, of which dimension of the cross section has 1.5 mm width (W), 30 mm length and 0.05 mm height (H) (Fig. 2). The flow path is constructed between parallel plates: the upper plate of polydimethylsiloxane (PDMS), and the lower plate of glass (S1111, Matsunami Glass, Japan). The upper plate has two holes of 5 mm diameter for the inlet and for the outlet of the flow of the cell suspension.

The micro pattern for the micro slit was controlled by two photomasks, which is made by the following process.

Photomask

The slide glass (Matsunami) plate (38 mm length, 26 mm width, and 1.0 mm thickness) was used for the base of the photomask (Fig. 3). Before the deposition of titanium, the surface of the glass plate was hydrophilized by the oxygen (30 cm^3/min, 0.1

Pa) plasma ashing for five minutes at 100 W by the reactive ion etching system (FA-1, Samco International, Kyoto, Japan). Titanium was deposited on the surface of the glass plate with 100 nm thickness in the electron beam vapor deposition apparatus (3.1×10^{-4} Pa, 0.5 nm/s, 200 s, JBS-Z0501EVC JEOL Ltd., Tokyo, Japan). The oxygen (0.1 Pa, 30 cm^3/min) ashing was applied on the surface of the titanium in the reactive ion etching system (100 W, for five minutes, FA-1).

To improve affinity between glass and photoresist material, HMDS (hexamethyldisilazane: Tokyo Chemical Industry Co., Ltd., Tokyo) was coated on the glass plate at 3000 rpm for 30 s with a spin coater. The positive photoresist material of OFPR-800LB (Tokyo Ohka Kogyo Co., Ltd, Tokyo, Japan) was coated on the titanium with the spin coater (at 5000 rpm for 30 s). The photoresist was baked in the oven (DX401, Yamato Scientific Co., Ltd) at 373 K for one minute.

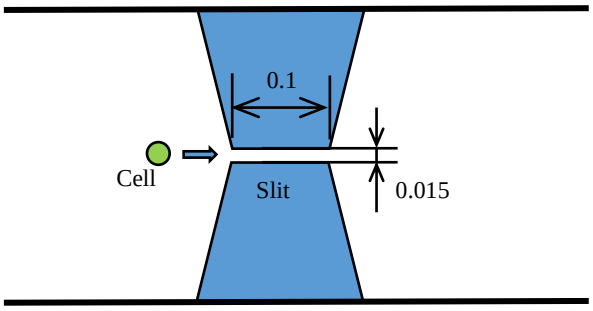

Fig. 1: Micro slit: unit of number, mm.

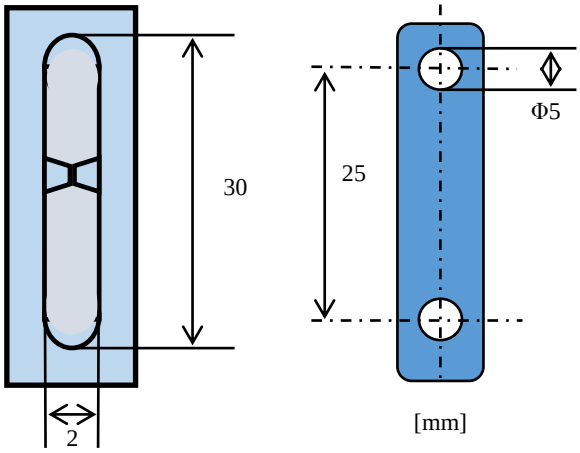

Fig. 2: Dimension of flow channel.

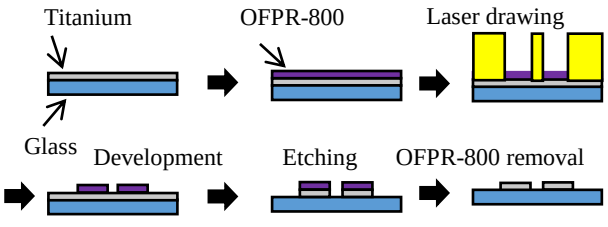

Fig. 3: Photolithography process for photomask.

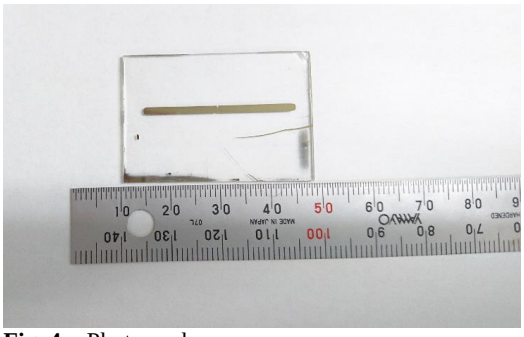

Fig. 4a: Photomask.

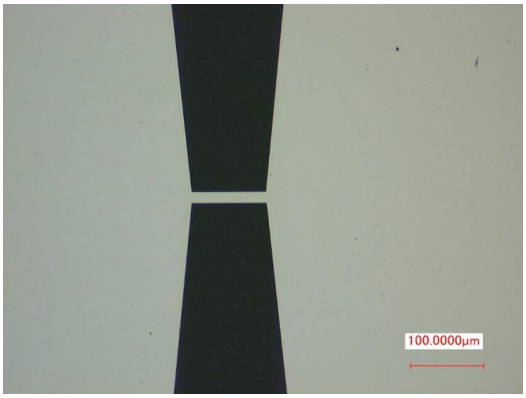

Fig. 4b: Magnified photomask at slit: dimension from left to right is 0.7 mm.

The pattern for the slit was drawn on the mask with a laser drawing system (DDB-201K-KH, Neoark Corporation, Hachioji, Japan). To control the dimension of the pattern on the mold with the laser drawing system, the parameters were selected as follows: the voltage of 3.2 V, the velocity of 0.151 mm/s, the acceleration of 0.34 mm/s^2, and the focus offset at +0.45.

The photoresist was developed with tetra-methyl-ammonium hydroxide (NMD-3, Tokyo Ohka Kogyo Co., Ltd., Kawasaki, Japan) for one minute, rinsed with the distilled water, and dried by the spin-dryer (1100 rpm, 30 s, with N_2 gas, SF-250, Japan Create Co., Ltd., Tokorozawa, Japan).

The titanium coated plate was etched with the plasma gas using RIE-10NR (Samco International, Kyoto, Japan). For etching, the gas of SF_6 (50 cm^3/min at 1013 hPa) with Ar (50 cm^3/min at 1013 hPa) was applied at 100 W at 4 Pa for five minutes. The residual OFPR-800LB was removed by acetone. The plate was dipped in the distilled water in one minute, after it is dipped in ethanol for one minute. The plate was dried by the spin-dryer: 300 rpm for 30 s with the distilled water, and 1100 rpm for 30 s with N_2 gas (Fig. 4).

Slit on Lower Plate

The glass slide was used for the base of micro slit, after cleaning with acetone (Fig. 5). The surface of the glass plate was hydrophilized by the oxygen (30 cm^3/min, 0.1 Pa) plasma ashing for five minutes at 100 W by the reactive ion etching system (FA-1). The negative photoresist material of high viscosity (SU8-10: Micro Chem Corp., MA, USA) was coated on the glass slide at 3000 rpm for 30 s with a spin coater. The photoresist was baked in the oven at 338 K for three hours.

The photoresist was exposed to the UV light through the mask in the mask aligner (M-1S, Mikasa Co. Ltd., Japan) at 15 mW/cm^2 for 16 s. The photoresist was baked at the hotplate in two processes: at 338 K for one minute, and at 368 K for ten minutes. The photoresist was developed with SU-8 Developer (Micro Chem) for ten minutes. The glass surface with the micro pattern was rinsed with IPA (2-propanol, Wako Pure Chemical Industries, Ltd.) for one minute, and pure water for one minute. The pattern was baked at the hotplate at 393 K (Fig. 6).

At the end of the process, the dimension of the micro pattern was measured with a Stylus Profiler (Dektak XT-E, Bruker Corporation). The height along the cross sectional line of micro pattern was traced (Fig. 7).

Upper Plate

After the slide glass plate was enclosed with a peripheral wall of polyimide tape, PDMS (Sylgard 184 Silicone Elastomer Base, Dow Corning Corp., MI, USA) was poured with the curing agent (Sylgard 184 Silicone Elastomer Curing Agent, Dow Corning Corp., MI, USA) on the mold. The volume ratio of PDMS to curing agent is ten to one. After degassing, PDMS was baked at 368 K for one hour in an oven (DX401, Yamato Scientific Co., Ltd). The baked plate of PDMS (3 mm thickness) was exfoliated from the slide glass plate. The PDMS plate was cut to make a rectangular upper plate for the flow channel. Two holes with the interval of 25 mm were punched by a punching tool (trepan MK405, Kai Industries Co., Ltd., Gifu, Japan) to make the inlet and the outlet. The upper plate was stuck on the lower plate with micro pattern adjusting the position of holes to make the flow channel. A rectangular parallelepiped channel of 30 mm length × 2 mm width × 0.05 mm height is formed between upper and lower plates. The two plates stick together with their surface affinity (Fig. 8).

A one-way flow system has been designed to introduce the suspension of cells. The system consists of a flow channel, tubes and a microscope. A silicone tube of 3 mm internal diameter and of 5 mm external diameter is used for the connector to the flow channel. The flow channel is placed on the stage of the inverted phase contrast microscope (IX71, Olympus Co., Ltd., Tokyo) (Fig. 9).

Flow Test

Cells of the passage between four and nine were used in the test. Three types of biological cells were used in the test alternatively: C2C12 (mouse myoblast cell line originated with cross-striated muscle of C3H mouse), Hepa1-6 (mouse hepatoma cell line of C57L mouse), or Neuro-2a (a mouse neural crest-derived cell line). The flow channel was hydrophilized by the oxygen (30 cm^3/min, 0.1 Pa) plasma ashing for one minute at 100 W by RIE (FA-1), and prefilled with the saline solution.

Before the flow test, the cells were exfoliated from the plate of the culture dish with trypsin, and suspended in the D-MEM (Dulbecco's Modified Eagle's Medium).

The flow path was carefully examined to avoid mixing of air bubbles, which might stir the medium in the flow channel. The suspension of cells (50 mm^3) was injected into the inlet of the flow channel, and introduced into the slits by the pressure difference between the inlet and the outlet, which was kept by the gravitational level of the medium (2.5 mm).

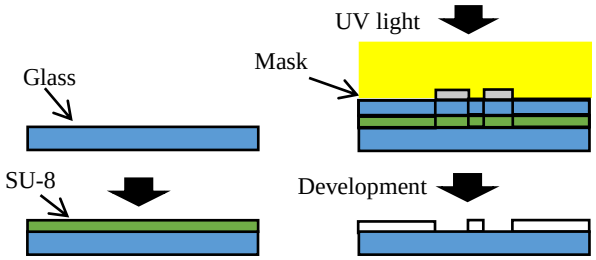

Fig. 5: Photolithography process for lower plate.

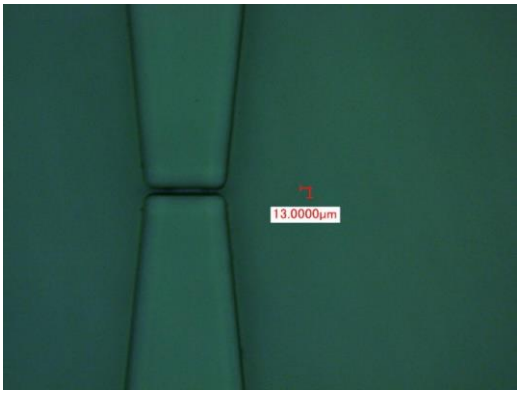

Fig. 6: Optical microscopic image of slit of SU8: dimension from left to right is 0.7 mm.

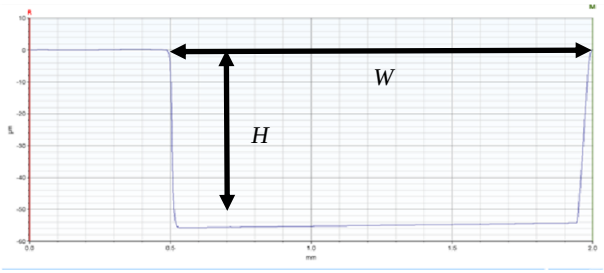

Fig. 7: Tracings of height of surface of lower plate of flow channel: *H*=0.05 mm, *W*=1.5 mm.

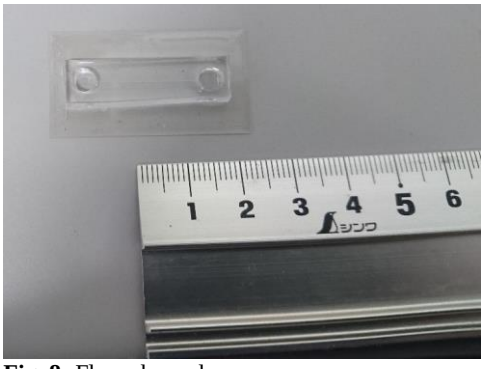

Fig. 8: Flow channel.

The cell passing through the slit was observed by the microscope, and recorded by the camera (DSC-RX100M4, Sony Corporation, Japan), which is set at the eyepiece. The movement of the cell was analyzed by Kinovea (Ver. 8.23, Commons Attribution) at the video images: 30 frames per second.

The deformation of the cell in the slit was calculated by the following equations (Fig. 10).

$$Q = v\,A = v\,(D_1\,H) \quad (1)$$
$$F = \rho\,Q\,v \quad (2)$$
$$S = \pi\,(D_0 / 2)^2 \quad (3)$$
$$\sigma = F / S \quad (4)$$
$$\varepsilon = (D_0 - D_1) / D_0 \quad (5)$$
$$E = \sigma / \varepsilon = \rho\,(D_1\,H)\,v^2 / (\pi\,(D_0 / 2)^2\,(D_0 - D_1) / D_0) \quad (6)$$

Where Q is the flow rate in the slit, v is the flow velocity in the slit, A is the cross sectional area of the slit, H is the height of the slit (5×10^{-5} m), F is force applied on the cell, ρ is the density of the fluid (1.0×10^3 kg/m^3), S is the cross section of the cell, σ is the stress applied on the cell, D_0 is the initial diameter of the cell, D_1 is the width of the slit, ε is the strain of the cell, and E is the elastic modulus.

3. RESULTS

Fig. 4 shows the photomask for the flow channel and the slit. The designed pattern is successfully etched on the titanium film on the glass. Fig. 6 shows the optical microscopic image of the slit. After adjustment of the micromachining condition, the designed pattern is successfully made on the glass. Fig. 7 shows the tracings of lower plate along the cross section of the micro-machined flow channel on the glass. The depth of the groove on the lower plate is 0.054 mm, which can be adjusted to the height of the micro slit of 0.05 mm (H) in the flow channel assembly. Fig. 8 shows the assembly of the upper and lower plate to make the flow channel.

Fig. 11 exemplifies C2C12 passing through the slit. Fig. 12 shows velocity of C2C12 passing through the slit. The zero velocity for four seconds corresponds to the movement of the cell attacking at the entrance of the slit. In this case, $E = 3 \times 10^{-2}$ Pa, calculated by $D_0 = 1.6 \times 10^{-5}$ m, $D_1 = 1.3 \times 10^{-5}$ m ($\varepsilon = 0.2$), $v = 1.4 \times 10^{-3}$ m/s.

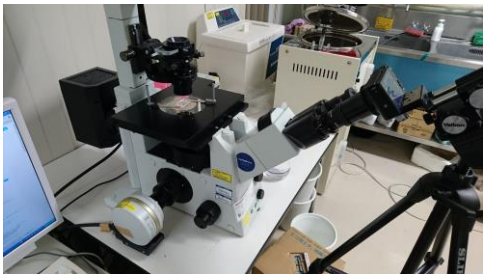

Fig. 9: Experimental system.

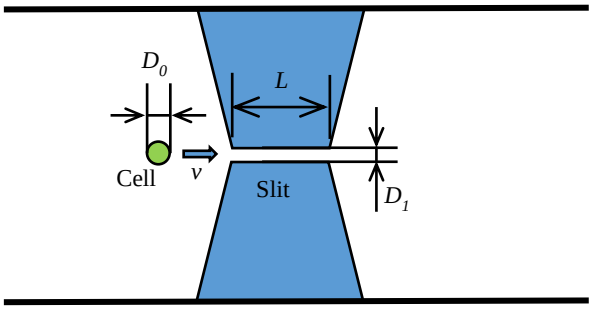

Fig. 10: Deformation of cell passing through slit.

Fig. 13 exemplifies Hepa1-6 passing through the slit. Fig. 14 shows velocity of Hepa1-6 passing through the slit. In this case, $E = 1 \times 10^{-2}$ Pa, calculated by $D_0 = 2.1 \times 10^{-5}$ m, $D_1 = 1.4 \times 10^{-5}$ m ($\varepsilon = 0.5$), $v = 1.4 \times 10^{-3}$ m/s.

Fig. 15 exemplifies Neuro-2a passing through the slit. Fig. 16 shows velocity of Neuro-2a passing through the slit. In this case, $E = 2 \times 10^{-4}$ Pa, calculated by $D_0 = 4.2 \times 10^{-5}$ m, $D_1 = 1.2 \times 10^{-5}$ m ($\varepsilon = 0.7$), $v = 0.6 \times 10^{-3}$ m/s.

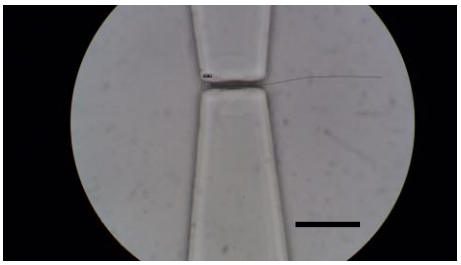

Fig. 11: C2C12 through slit: flow from left to right, bar shows 0.1 mm.

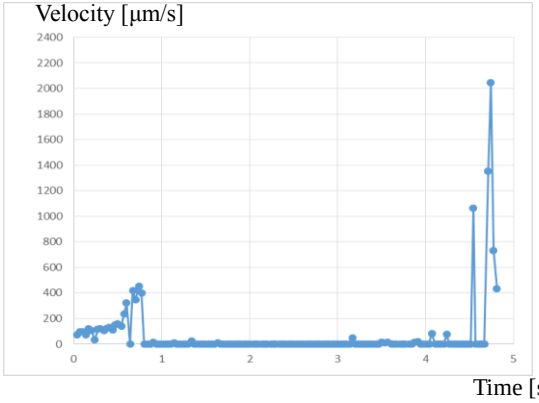

Fig. 12: Velocity of C2C12 passing through slit.

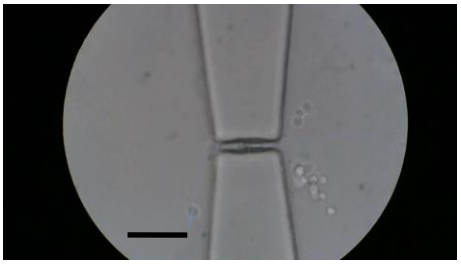

Fig. 13: Hepa1-6 through slit: flow from left to right, bar shows 0.1 mm.

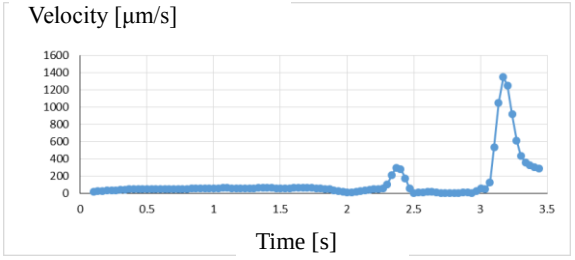

Fig. 14: Velocity of Hepa1-6 passing through slit.

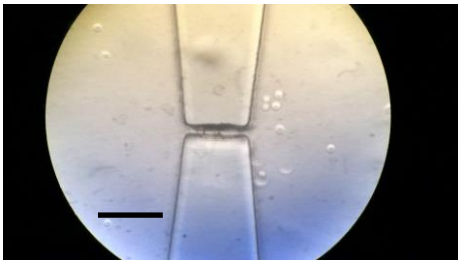

Fig. 15: Neuro-2a through slit: flow from left to right, bar shows 0.1 mm.

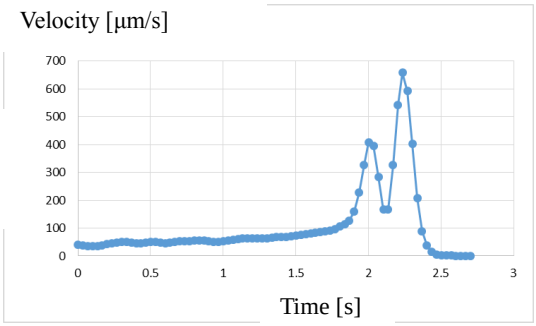

Fig. 16: Velocity of Neuro-2a passing through slit.

4. DISCUSSION

Preparation of the slit of sub-micrometer is not easy. In the previous study, the slit of micrometer between pillars was manufactured by photolithography technique [1]. In another study, the micro slit was manufactured between ridges [2]. Only one projection can be traced in the present experimental system. The cell can deform in the perpendicular direction. To observe the deformation in the perpendicular plane, the slit between upper and lower ridges is effective [2].

There are several methods to sort cells [3-10]. Non-invasive way is preferable to sort cells with minimum damage. The flow cytometry is one of the technologies, which is used for cell sorting. Cells suspended in the fluid are analyzed by the laser. The fluorescently labelled components in the cell are analyzed by the light emission. The experimental results might contribute to analyze adhesive mechanism of cancer cell during metastasis. The micro trap might simulate adhesive mechanism of flowing cells.

A red blood cell has flexibility and deforms in the shear flow [22, 23]. It also passes through micro-circulation, of which the dimension is smaller than the diameter of the red blood cell. After circulation through the blood vessels for days, the red blood cell is trapped in the micro-circulation systems.

In the previous study, several slits were designed between micro columns [1]. The multiple slits are convenient to sort cells as the filter. The fluid selected, however, a slit of parallel multiple slits at random in the previous system. While a cell is passing through a slit, the main fluid flows through another slit. The driving force of the passing cell changes with the clogging at the slit.

The resistance of the flow channel with a single slit is very high in the present experimental system. The resistance increases, when the cells clogged the slits in the flow channel. Internal pressure of the flow channel should be carefully controlled under the constant flow rate, otherwise the leakage or cavitation would occur. In the present study, the flow rate is confirmed by the flow speed of the cell during microscopic observation.

The optical micro scope observation is difficult at the tall slit with the narrow width, because of the scattering of the light. The height of the wall is limited to 0.05 mm in the present study. The wall of the flow channel has the taper to introduce cells smoothly to the single slit in the present study. Although the dimension of the width of the slits (D_1) was scattered between 0.012 mm and 0.014 mm, the morphology of the micro pattern has been successfully manufactured by the photolithography process in the present study.

The high speed camera is necessary to trace the deformation of a cell in the slit, because the cell slips fast after entering into the slit. In some cases, on the other hand, it takes time to deform from sphere to disk to enter into the slit.

The capture of the cell at the slit depends on several factors: the dimension of the cell and the slit, deformability of the cell, the wall shear stress (shear rate) at the slit, and the affinity (charge, friction) of the cell to the wall of the slit. The surface is not completely flat in the slit, which might make frictional resistance. Protein coating might make property of the surface stable.

According to the experimental results of in the present study, the ascending order of compliance of the cell estimated by the elastic modulus is C2C12, Hepa1-6, Neuro-2a. Hepa1-6 is able to pass the narrower slit than C2C12.

5. CONCLUSION

A single micro slit has been designed between walls to observe the deformation of a cell passing through the slit. The micro slit of 0.015 mm width, 0.1 mm length and 0.05 mm height was fabricated between walls of weirs on the glass plate using the photolithography technique. The suspension of cells (C2C12 or Hepa1-6) was introduced into the slits, and the cell passing through the slit was observed by the microscope. Both the movement and the shape of the cell were analyzed at the video images. The elastic modulus of myoblast passing through the slit estimated by the velocity (1 mm/s) and by the deformation (0.5) of the cell in the slit was 10^{-2} Pa. The experimental results show that the designed slit has capability to measure deformability of the cell.

6. ACKNOWLEDGMENT

This work was supported by a Grant-in-Aid for Strategic Research Foundation at Private Universities from the Japanese Ministry of Education, Culture, Sports and Technology.

REFERENCES

[1] Y. Takahashi, S. Hashimoto, H. Hino and T. Azuma, “Design of Slit between Micro Cylindrical Pillars for Cell Sorting”, **Journal of Systemics, Cybernetics and Informatics**, Vol. 14, No. 6, 2016, pp. 8-14.

[2] A. Mizoi, Y. Takahashi, H. Hino, S. Hashimoto and T. Yasuda, "Deformation of Cell Passing through Micro Slit between Micro Ridges", **Proc. 20th World Multi-Conference on Systemics Cybernetics and Informatics**, Vol. 2, 2016, pp. 129-134.

[3] J.C. Baret, O.J. Miller, V. Taly, M. Ryckelynck, A. El-Harrak, L. Frenz, C. Rick, M.L. Samuels, J.B. Hutchison, J.J. Agresti, D.R. Link, D.A. Weitz and A.D. Griffiths, "Fluorescence -activated Droplet Sorting (FADS): Efficient Microfluidic Cell Sorting Based on Enzymatic Activity", **Lab on a Chip**, Vol. 9, No. 13, 2009, pp. 1850-1858.

[4] A. Khademhosseini, J. Yeh, S. Jon, G. Eng, K.Y. Suh, J.A. Burdick and R. Langer, "Molded Polyethylene Glycol Microstructures for Capturing Cells within Microfluidic Channels", **Lab on a Chip**, Vol. 4, No. 5, 2004, pp. 425-430.

[5] M. Yamada and M. Seki, "Hydrodynamic Filtration for On-chip Particle Concentration and Classification Utilizing Microfluidics", **Lab on a Chip**, Vol. 5, No. 11, 2005, pp. 1233-1239.

[6] S.C. Hur, N.K. Henderson-Maclennan, E.R.B. McCabe and D.D. Carlo, "Deformability-based Cell Classification and Enrichment Using Inertial Microfluidics", **Lab on a Chip**, Vol. 11, No. 5, 2011, pp. 912-920.

[7] A.A. Bhagat, H. Bow, H.W. Hou, S.J. Tan, J. Han and C.T. Lim, "Microfluidics for Cell Separation", **Medical & Biological & Engineering & Computing**, Vol. 48, No. 10, 2010, pp. 999-1014.

[8] D.R. Gossett, W.M. Weaver, A.J. Mach, S.C. Hur, H.T.K. Tse, W. Lee, H. Amini and D.D. Carlo, "Label-free Cell Separation and Sorting in Microfluidic Systems", **Analytical and Bioanalytical Chemistry**, Vol. 397, No. 8, 2010, pp. 3249–3267.

[9] S.M. McFaul, B.K. Lin and H. Ma, "Cell Separation Based on Size and Deformability Using Microfluidic Funnel Ratchets", **Lab on a Chip**, Vol. 12, No. 13, 2012, pp. 2369-2376.

[10] L.R. Huang, E.C. Cox, R.H. Austin and J.C. Sturm, "Continuous Particle Separation through Deterministic Lateral Displacement", **Science**, Vol. 304, No. 5673, 2004, pp. 987-990.

[11] Y. Takahashi, S. Hashimoto, H. Hino, A. Mizoi and N. Noguchi, "Micro Groove for Trapping of Flowing Cell", **Journal of Systemics, Cybernetics and Informatics**, Vol. 13, No. 3, 2015, pp. 1-8.

[12] A.Y. Fu, C. Spence, A. Scherer, F.H. Arnold and S.R. Quake, "A Microfabricated Fluorescence-Activated Cell Sorter", **Nature Biotechnology**, Vol. 17, 1999, pp. 1109-1111.

[13] Y.C. Ou, C.W. Hsu, L.J. Yang, H.C. Han, Y.W. Liu and C.Y. Chen, "Attachment of Tumor Cells to the Micropatterns of Glutaraldehyde (GA)-Crosslinked Gelatin", **Sensors and Materials**, Vol. 20, No. 8, 2008, pp. 435-446.

[14] G.L. Hart, M. Wortis and R. Mukhopadhyay, "Stomatocyte-discocyte-echinocyte Sequence of the Human Red Blood Cell: Evidence for the Bilayer Couple Hypothesis from Membrane Mechanics" , **Proceedings of the National Academy of Science of the United States of America**, Vol. 99, No. 26, 2002, pp. 16766-16769.

[15] K. Takahashi and S. Yamanaka, "Induction of Pluripotent Stem Cells from Mouse Embryonic and Adult Fibroblast Cultures by Defined Factors", **Cell**, Vol. 126, No. 4, 2006, pp. 663-676.

[16] H.M. Ji, V. Samper, Y. Chen, C.K. Heng, T.M. Lim and L. Yobas, "Silicon-based Microfilters for Whole Blood Cell Separation", **Biomedical Microdevices**, Vol. 10, 2008, pp. 251–257.

[17] H.W. Hou, Q.S. Li, G.Y.H. Lee, A.P. Kumar, C.N. Ong and C.T. Lim, "Deformability Study of Breast Cancer Cells Using Microfluidics", **Biomedical Microdevices**, Vol. 11, No. 3, 2009, pp. 557-564.

[18] M.R. King, L.T. Western, K. Rana and J.L. Liesveld, "Biomolecular Surfaces for the Capture and Reprogramming of Circulating Tumor Cells", **Journal of Bionic Engineering**, 2009, Vol. 6, No. 4, pp. 311-317.

[19] H.W. Hou, A.A.S. Bhagat, A.G.L. Chong, P. Mao, K.S.W. Tan, J. Han and C.T. Lim, "Deformability Based Cell Margination — A Simple Microfluidic Design for Malaria-infected Erythrocyte Separation", **Lab on a Chip**, Vol. 10, No. 19, 2010, pp. 2605-2613.

[20] S.K. Lee, G.S. Kim, Y. Wu, D.J. Kim, Y. Lu, M. Kwak, L. Han, J.H. Hyung, J.K. Seol, C. Sander, A. Gonzalez, J. Li and R. Fan, "Nanowire Substrate-based Laser Scanning Cytometry for Quantitation of Circulating Tumor Cells", **Nano Letters**, Vol. 12, No. 6, 2012, pp. 2697-2704.

[21] W. Zhang, K. Kai, D.S. Choi, T. Iwamoto, Y.H. Nguyen, H. Wong, M.D. Landis, N.T. Ueno, J. Chang and L. Qin, "Microfluidics Separation Reveals the Stem-cell-like Deformability of Tumor-initiating Cells", **Proceedings of the National Academy of Science**, Vol. 109, No. 46, 2012, pp. 18707-18712.

[22] S. Hashimoto, et al., "Effect of Aging on Deformability of Erythrocytes in Shear Flow", **Journal of Systemics, Cybernetics and Informatics**, Vol. 3, No. 1, 2005, pp. 90-93.

[23] S. Hashimoto, "Detect of Sublethal Damage with Cyclic Deformation of Erythrocyte in Shear Flow", **Journal of Systemics Cybernetics and Informatics,** Vol. 12, No. 3, 2014, pp. 41-46.

[24] H. Hino, S. Hashimoto and F. Sato, "Effect of Micro Ridges on Orientation of Cultured Cell", **Journal of Systemics Cybernetics and Informatics,** Vol. 12, No. 3, 2014, pp. 47-53.

[25] B. Bohl, R. Steger, R. Zengerle and P. Koltay, "Multi-layer SU-8 Lift-off Technology for Microfluidic Devices", **Journal of Micromechanics and Microengineering**, Vol. 15, No. 6, 2005, pp. 1125-1130.

[26] Y. Song, C.S.S.R. Kumar and J. Hormes, "Fabrication of an SU-8 Based Microfluidic Reactor on a PEEK Substrate Sealed by a 'Flexible Semi-solid Transfer' (FST) Process", **Journal of Micromechanics and Microengineering**, Vol. 14, No. 7, 2004, pp. 932-940.

[27] J. Friend and L. Yeo, "Fabrication of Microfluidic Devices Using Polydimethylsiloxane", **Biomicrofluidics**, Vol. 4, No. 4, 2010, pp. 26052-26057.